

# Wafer-Scale High-Throughput Ordered Growth of Vertically Aligned ZnO Nanowire Arrays

Yaguang Wei,<sup>†,§</sup> Wenzhuo Wu,<sup>†,§</sup> Rui Guo,<sup>†</sup> Dajun Yuan,<sup>†</sup> Suman Das,<sup>\*,†</sup> and Zhong Lin Wang<sup>\*,†</sup>

<sup>†</sup>School of Materials Science and Engineering and <sup>‡</sup>Woodruff School of Mechanical Engineering, Georgia Institute of Technology, Atlanta, Georgia 30332-0245

**ABSTRACT** This article presents an effective approach for patterned growth of vertically aligned ZnO nanowire (NW) arrays with high throughput and low cost at wafer scale without using cleanroom technology. Periodic hole patterns are generated using laser interference lithography on substrates coated with the photoresist SU-8. ZnO NWs are selectively grown through the holes via a low-temperature hydrothermal method without using a catalyst and with a superior control over orientation, location/density, and as-synthesized morphology. The development of textured ZnO seed layers for replacing single crystalline GaN and ZnO substrates extends the large-scale fabrication of vertically aligned ZnO NW arrays on substrates of other materials, such as polymers, Si, and glass. This combined approach demonstrates a novel method of manufacturing large-scale patterned one-dimensional nanostructures on various substrates for applications in energy harvesting, sensing, optoelectronics, and electronic devices.

**KEYWORDS** ZnO, nanowire, arrays, laser interference lithography, nanofabrication

ZnO nanowire (NW) is one of the most important one-dimensional nanostructured building blocks for energy harvesting,<sup>1–5</sup> sensing,<sup>6,7</sup> optoelectronic,<sup>8,9</sup> and electronic<sup>10,11</sup> applications. Assembly and integration of highly ordered NW arrays in large scale is essential for multifunctional devices and systems.<sup>12–14</sup> Significant efforts have been made to assemble large quantity NWs through parallel processes, which can be grouped into two categories: grow-and-place (GAP) and grow-in-place (GIP). The GAP approach includes but is not limited to alignment induced by dielectrophoresis<sup>15</sup> and methods utilizing magnetic fields<sup>16</sup> as well as microfluidic,<sup>17</sup> electrostatic,<sup>18</sup> molecular,<sup>19</sup> and shear forces.<sup>20–22</sup> Although the GAP technique can be used to fabricate a finite number of devices, it is rather challenging to assemble the as-synthesized NWs into desired configurations in large scale. In GIP technique, nanostructures grow in situ at the patterned catalyst/seed sites created through lithography, such as electron beam lithography (EBL),<sup>23</sup> nanoimprint lithography (NIL),<sup>24</sup> and nanosphere lithography (NSL).<sup>25</sup> Control over the growth substrate can guide the size, placement, and orientation of the grown NWs. Patterned growth of aligned ZnO NWs has been achieved via hydrothermal (HT) method<sup>23</sup> and physical vapor deposition (PVD).<sup>25</sup> However, none of the above approaches provides a reliable, high-throughput, and low-cost solution for large-

scale fabrication of patterned ZnO NW arrays at a level required for industrial applications.

To achieve controllable growth of highly ordered and aligned ZnO NW arrays with high throughput and low cost in large scale, it is necessary to adopt feasible combinations of patterning techniques and ZnO NWs synthesis methods. In this letter, we demonstrate one such approach for patterned growth of vertically aligned ZnO nanowire arrays by combining laser interference lithography (LIL),<sup>26</sup> which is a large-scale, fast, maskless, and noncontact nanopatterning technique and HT growth of ZnO NWs<sup>27</sup> either homoepitaxially on textured ZnO layer, which is also synthesized wet-chemically, or heteroepitaxially on GaN film. The substrates can be patterned with periodic ordered, variable spacing, and symmetry over large areas of up to a 2 in. wafer by LIL. Perfectly aligned vertical ZnO NW arrays were then grown at predefined positions via a low-temperature HT method without using a catalyst but with control over orientation, dimension, and location. As-synthesized NWs are highly uniform in length and diameter with perfect alignment and are single crystals with growth direction along [0001].

The patterns for synthesis of ZnO NW arrays were prepared by LIL of the photoresist, which is a photochemical process similar to that in the state-of-the-art photolithography process. The epoxy-based negative photoresist SU-8, commonly used in the microelectronics industry, was adopted in our experiment. The LIL technique generates patterns on the photoresist masklessly. When exposed, SU-8's long molecular chains cross-link and cause the solidification of the exposed areas. After development, the exposed areas of SU-8 layer remained and served as the mask for the

\* Corresponding authors. E-mail: zhong.wang@mse.gatech.edu (Z.L.W.), sumandas@gatech.edu (S.D.).

§ Authors contributed equally to this work.

Received for review: 4/22/2010

Published on Web: 08/03/2010



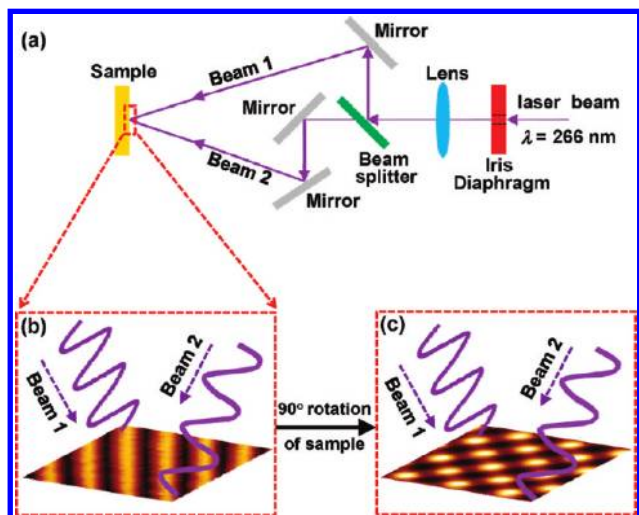


FIGURE 1. (a) Schematics of experimental setup for the laser interference patterning. A 10 ns pulsed Nd:YAG laser (Quanta-Ray PRO 290, Spectra Physics) with wavelength of 266 nm is used as the laser source. The primary laser beam (266 nm) was split into two coherent light beams (beams 1 and 2). (b) The interference between beam 1 and 2 formed a grating pattern on the photoresist layer under a single laser pulse (10 ns) irradiation. (c) The sample was then rotated by 90° or by an arbitrary angle with a second exposure, and patterns of periodic nanodot arrays were formed on the photoresist layer or the substrate. The grating and nanodot patterns in Figure 1b and c were fabricated on SU 8 via LIL approach and acquired by scanning probe microscope (Veeco Dimension 3100).

growth of ZnO NWs. The experimental setup for the laser interference patterning is shown in Figure 1a. A 10 ns pulsed Nd:YAG laser (Quanta-Ray PRO 290, Spectra Physics) with a wavelength of 266 nm is used as the laser source. The primary laser beam (266 nm) was split into two coherent light beams (Figure 1a). Interference between the beams formed a grating pattern (Figure 1b) on the photoresist layer under a single laser pulse (10 ns) irradiation. The period of the pattern line spacing  $d$  is determined by the wavelength ( $\lambda$ ) of the light and the half angle ( $\theta$ ) between the two incident beams through the relationship  $d = \lambda/2\sin(\theta)$ . The sample was then rotated by 90° followed by a second exposure, and patterns of periodic nanodot arrays were formed on the photoresist layer (Figure 1c).

Figure 2a presents the schematics of fabrication sequences of vertically aligned ZnO NW arrays using the laser interference technique. LIL technique was used for forming patterns on the SU-8 layer, in a way described in Figure 1. The negative photoresist SU-8 was spin coated onto a 2 in. silicon or sapphire wafer, on top of which is a layer of ZnO texture or GaN film with (0001) surface orientation, respectively. The pattern of open-hole arrays was formed uniformly at the unexposed locations of SU-8 layer over the whole wafer area after two consecutive laser exposures with 90° rotation of the substrate between exposures. As can be seen in Figure 2a, the (0001) surface of ZnO or GaN layer has been selectively exposed for the subsequent growth of aligned ZnO NW arrays. The substrate with patterned SU-8 layers was then put facing downward into the growth solution,

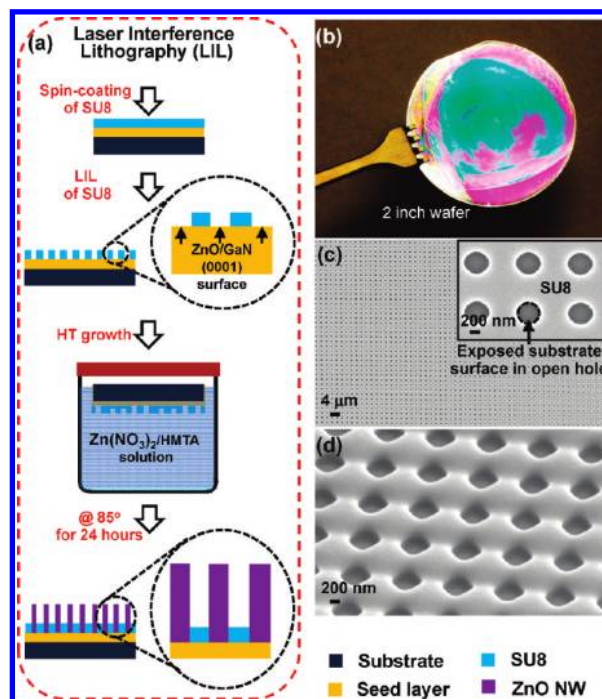
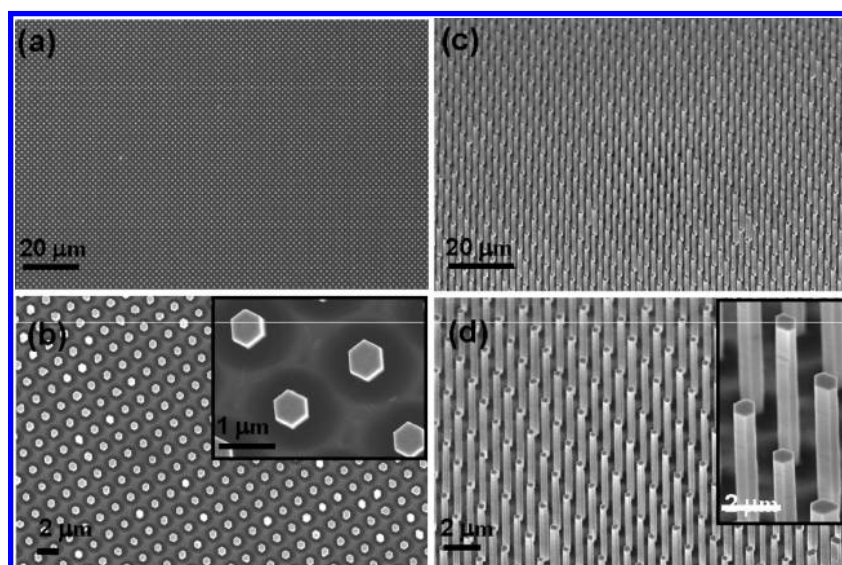


FIGURE 2. Schematics of the fabrication sequences of vertically aligned ZnO NW arrays using laser interference techniques. (a) Fabrication sequence using the LIL approach for large-scale patterned vertically aligned ZnO NW arrays. (b) Optical image of a 2 in. Si wafer with a SU-8 open-hole pattern over the whole surface area. The iridescence dispersion demonstrates the excellent periodicity over the entire wafer surface. (c) The top-view SEM image of patterned SU-8 film (thickness of 500 nm). Inset, top-view SEM image of patterned SU-8 film at higher magnification. The area encircled by the black dashed line is the exposed surface of substrate. (d) 45°-tilted-view SEM image of patterned SU-8 film.

floating on top of the nutrient solution surface for NWs growth. Vertically aligned ZnO NW arrays were synthesized in a solution containing 5 mM zinc nitride (Alfa Aesar) and 5 mM hexamethylenetetramine (HMTA) (Fluka) at 85 °C for 24 h in a Yamato convection box oven. ZnO NWs grew at the substrate sites not covered by the SU-8 layer, and uniformly patterned ZnO NW arrays were hence obtained in large scale. The morphology of ZnO NWs can be tuned by varying solution concentration, growth temperature, and time.<sup>27</sup> The perfectly vertical alignment of ZnO NW arrays was achieved due to the lattice match between the grown ZnO (0001) and substrate (either ZnO texture or GaN layer) planes. Both LIL and HT methods are carried out at low temperature (below 100 °C) and ambient pressure. It is straightforward to extend this approach to fabrication of nanostructure arrays of other materials like Si, CdSe, and III–V compounds on various other substrates, such as glass, flexible materials, and metals.

The formed patterns on SU-8-coated substrate after LIL patterning were imaged by a thermally assisted field emission scanning electron microscope (SEM) (LEO 1530), as shown in Figure 2. Figure 2b is the optical image of a 2 in. Si wafer with SU8 open-hole pattern over the whole surface area. Figure 2c is the top view of a patterned SU-8 film (500



**FIGURE 3.** The heteroepitaxial growth of vertically aligned ZnO NW arrays on GaN substrate via LIL approach. (a and b) Top-view SEM images of vertically aligned ZnO NW arrays on GaN substrate in large-scale uniform pattern at different magnifications. (c and d) 45°-tilted-view SEM images of vertically aligned ZnO NW arrays on GaN substrate in large-scale uniform pattern at different magnifications.

nm thick). The presented pattern has a period of  $2\ \mu\text{m}$ , and circular holes with diameter of  $600\ \text{nm}$  were opened over the surface uniformly with irradiation fluence of  $3.5\ \text{mJ}/\text{cm}^2$  for the laser beams. The sidewalls of the holes are approximately vertical, and the substrate was selectively exposed (top and 45°-tilted views in Figure 2c and d, respectively). The shapes, periods of the pattern, and scales of the hole can be adjusted by varying the laser interference patterning parameters, such as the fluence and the aperture size, and other experimental parameters like the angle of rotation applied to the samples between exposures. A detailed study on pattern generation will be discussed later in this article.

The heteroepitaxial growth of vertically aligned ZnO NW arrays on GaN substrate was investigated first. The morphology and uniformity of the patterned NW arrays via LIL approach were examined and confirmed by SEM images (Figure 3). Almost all of the NWs have the same diameter and height. The aligned ZnO NW arrays were uniformly grown following the patterned holes with high fidelity at diameter of  $\sim 600\ \text{nm}$  (Figure 3b). All the NWs are perfectly aligned normal to the substrate and have the same height of  $\sim 5\ \mu\text{m}$  (Figure 3c and d).

LIL patterned growth of ZnO NW arrays was also performed with different periods and sizes of opened holes (Supporting Information, Figure S1) on GaN substrate. An interesting phenomenon was observed when comparing the ZnO NW arrays for patterns with different diameters of holes. When the diameter of opened holes was smaller than  $600\ \text{nm}$  (Supporting Information, Figure S2a–d and Figure 3), an individual ZnO NW grew out of each hole. All of the NWs have perfect vertical alignment with the same diameter and height. When the diameter of opened holes is larger than  $1\ \mu\text{m}$ , random growth of ZnO NWs was observed (Support-

ing Information, Figure S2e–h) on the substrate with different diameters and heights for the grown ZnO NWs, which is similar to the result obtained for ZnO NWs growing on unpatterned bare GaN substrates. This selective area growth may be understood from the nucleation and growth processes. The nuclei form at the beginning of the growth, which initiates and guides the subsequent growth of NWs when the sizes of the nuclei exceed the critical size. A competition exists between the NW growth and the nucleus formation. The competition in open space leads to random growth of NW arrays due to its large size and multiple nucleations. When the surface for NW growth is confined in small areas separated at a certain distance from each other, one nucleus is formed in each confined spot, which then grows into a single NW. A 2-D model proposed by Coltrin et al.<sup>28</sup> also describes the selective area growth by introducing a diffusion mechanism of reaction byproduct in their model. The mechanism of selective area growth can be further investigated for different pattern dimensions using the LIL approach described above. A more in-depth understanding of selective area growth can enable fabricating large-scale patterned ZnO NW arrays in a more controllable way.

In order to achieve vertically aligned ZnO NW arrays, either by HT or physical vapor deposition method, matches in the crystallographic orientation and lattice parameter between the substrate material and the ZnO are required. Substrates, such as single crystalline GaN<sup>25</sup> or ZnO,<sup>29</sup> were previously adopted for the nanowire growth. However, the high cost of these substrates limits potential large-scale applications. Furthermore, applications using substrates of other materials, such as polymers and glass, have been of more interest due to cost and handling considerations. It is hence highly desirable to develop a general method for

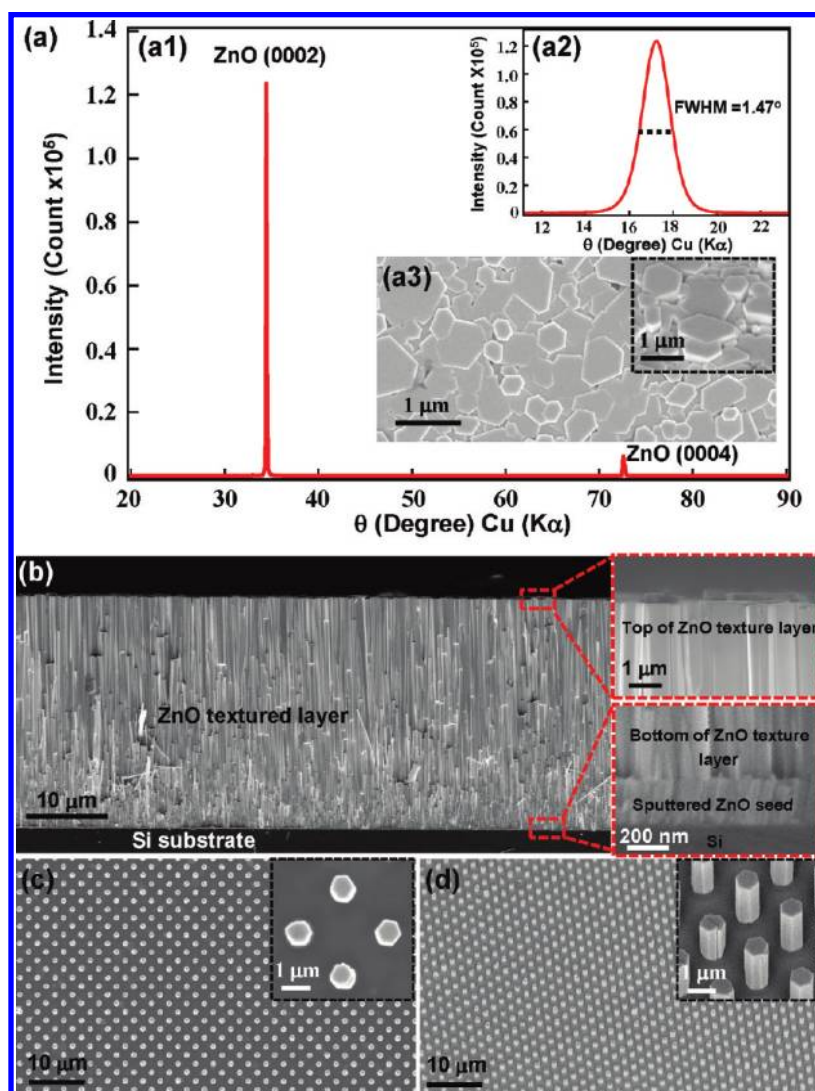


FIGURE 4. The homoepitaxial growth of large-scale vertically aligned ZnO NW arrays via LIL approach on textured ZnO seed layer. (a) XRD measurements investigating the crystal structure and orientation of the as-grown textured ZnO seed layer. (a1) The  $\theta-2\theta$  scan shows only two dominant peaks at  $34.45^\circ$  and  $72.59^\circ$ , attributed to the ZnO (0002) and (0004) planes, respectively. (a2) The  $\theta$  rocking curve of textured ZnO seed layer was also investigated for a peak at  $34.45^\circ$ , with a full width at half-maximum (fwhm) value of  $1.47^\circ$ . The small fwhm value indicates good alignment among different (0001) oriented domains of the textured ZnO seed layer. (a3) Insets are the top and  $45^\circ$ -tilted views of the as-prepared textured ZnO seed layer, respectively. The ZnO seed layer was formed by tightly compact ZnO NWs grown along [0001] direction. Those NWs have flat top (0001) surfaces and small variation in height steps (Figure 4a3 inset). (b) Cross-section of the as-grown dense textured ZnO layer. A layer of presputtered ZnO seed layer (around 200 nm thick, indicated in Figure 4b) on the supporting substrate was found to be necessary for growth of the dense textured ZnO layer. Height variations at the top surface of the as-grown dense textured ZnO layer are confirmed to be small. (c and d) Insets and top- and  $45^\circ$ -tilted-view SEM images of vertically aligned ZnO NW arrays on silicon substrate with a textured ZnO layer in large-scale uniform pattern at different magnifications.

fabricating vertically aligned ZnO NW arrays on essentially any substrate of low cost. The same LIL patterning and HT NW growth sequences were performed on a silicon wafer covered with a polycrystalline ZnO seed layer prepared by RF magnetron sputtering. Multiple ZnO NWs (Supporting Information, Figure S2) grew out of each hole due to the random in-plane orientations of the polycrystalline ZnO seeds deposited on the silicon wafer. A textured ZnO seed layer with a flat (0001) surface is hence desirable for subsequent growth of vertically aligned ZnO NW arrays, and we developed a simple way to prepare large-scale textured ZnO seed layers with a flat (0001) surface at low cost.

First, the silicon wafer was sputtered with a layer of ZnO with a thickness around 200 nm (Figure 4b) in a RF magnetron sputtering system. The wafer was then put facing downward into the growth solution, floating on top of the nutrient solution surface for growth. A dense layer of aligned ZnO NWs were synthesized in a solution containing 20 mM zinc chloride ( $\text{ZnCl}_2$ ) and 20 mM HMTA at  $95^\circ\text{C}$  for 16 h in a Yamato convection box oven. Ammonium hydroxide ( $\text{NH}_4\text{OH}$ ) was also added into the solution at a volume concentration of around 4%. The cross-section of this dense layer of aligned ZnO NWs was shown in Figure 4b. Figure 4a3 and its inset are the top and  $45^\circ$ -tilted views of an as-

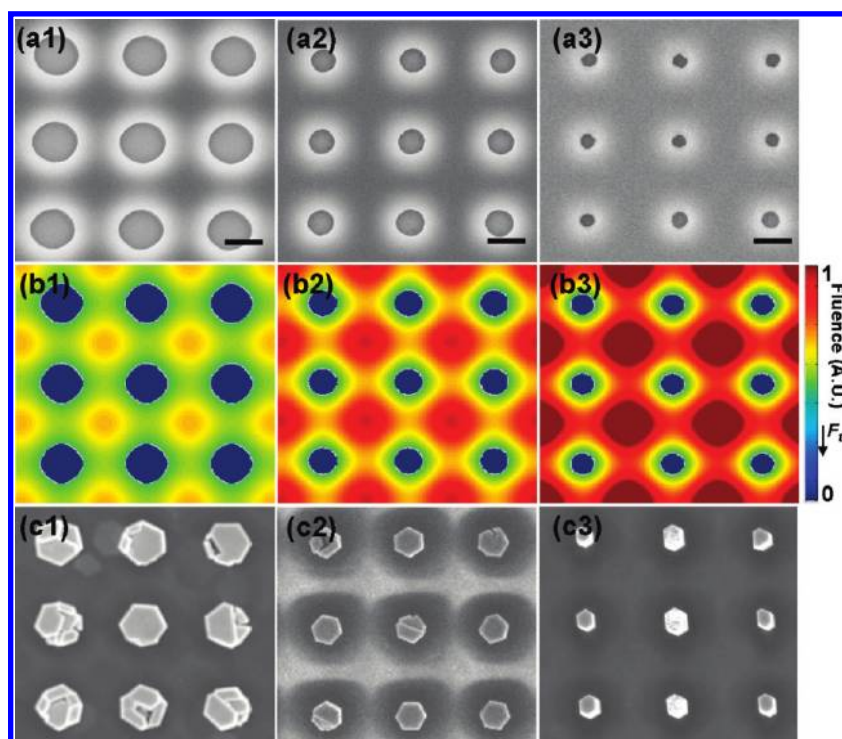


FIGURE 5. (a1–a3) Top-view SEM images of SU-8 patterns of different hole opening sizes on Si substrate with textured ZnO seed layer with the interference light fluence of 1.6, 3.2, and 6.0 mJ/cm<sup>2</sup>, respectively. (b1–b3) Simulated laser fluence distribution in SU-8 using the same laser fluencies as those in a1–a3. (c1–c3) Top-view SEM images of vertically aligned ZnO NW arrays, which follow the predefined pattern of SU-8 layer with high fidelity.

prepared textured ZnO seed layer, respectively. The ZnO seed layer was formed by tightly compact ZnO NWs grown along a [0001] direction. Those NWs have flat top (0001) surfaces (Figure 4a3) and small variation in height steps (Figure 4a3 inset and b). The crystal structure and orientation of the as-grown textured ZnO seed layer were studied by X-ray diffraction (XRD) measurements. The XRD  $\theta$ – $2\theta$  scan (Figure 4a1) shows only two dominant peaks at 34.45° and 72.59°, attributed to the ZnO (0002) and ZnO (0004) planes, respectively. The XRD  $\theta$ – $2\theta$  scan indicates that the surface of textured ZnO seed layer is (0001) oriented. The XRD  $\theta$  rocking curve (Figure 4a2) of textured ZnO seed layer was also investigated for a peak at 34.45°, with a full width at half-maximum (FWHM) value of 1.47°. The small FWHM value indicates good alignment among different (0001) oriented domains of the textured ZnO seed layer.

The textured ZnO seed layer was then used for the growth of vertically aligned ZnO NWs via LIL patterning and the HT NW growth sequences described previously. The perfectly vertical alignment of ZnO NW arrays was homoepitaxially achieved (Figure 4c and d) due to ideal match between the (0001) facets of the dense ZnO NWs achieved in the first growth process and the ZnO NWs grown on top of them during the second growth process. The hexagonal shape of the NW indicates that it is a single crystal with growth direction along [0001]. The NWs have the same diameter of around 1  $\mu$ m. All of the NWs are perfectly aligned normal to the substrate and have the same height of around 2  $\mu$ m.

The hole diameter and periodicity can be controlled by varying the fluence of the primary laser beam and the angle between the interfering beams, respectively. We studied the growth of ZnO NW arrays with different hole diameters on Si substrate with a textured ZnO seed layer. Patterns with a fixed period of 2.5  $\mu$ m but with varying hole diameters were obtained at a fixed angle of 6.3° between the interfering beams. The diameters of the holes are 1  $\mu$ m and 700 and 350 nm, respectively, in Figure 5a1–a3, which were generated at fluencies of 1.6, 3.2, and 6.0 mJ/cm<sup>2</sup>, respectively. For a negative photoresist, the hole diameter decreases with increasing exposure dose. The fluence distribution on the SU-8 substrate after two successive patterning exposures was simulated using the same exposure parameters as those in Figure 5a1–a3. Figure 5b1–b3 shows the corresponding calculated fluence distribution, through which the holes are created at the locations where the exposure dose is lower than the threshold fluence ( $F_{th}$ ) for photocuring of SU-8, shown as the circular areas in dark blue in all three simulated results. SU-8 will not be photocured in these areas and hence will be dissolved in the subsequent developing process to holes. The simulation results are in good agreement with the experimental results, as shown here in Figure 5. Synthesis of vertically aligned ZnO NW arrays was then carried out, and the results are shown in Figure 5c1–c3. It can be seen that the as-grown NW arrays follow the predefined pattern of SU-8 layer with high-fidelity. When the hole size is large (1  $\mu$ m), distinct boundaries can be observed in grown NWs,

which are attributed to the finite size of the domains in the underneath ZnO texture layer (Figure 4a3). Fewer boundaries exist with decreased size of hole openings. It is observed that when the hole size lies below the average domain size in the underneath ZnO texture layer (around 500 nm), single intact ZnO NW grows out of each hole without any boundaries observed at the top facet (Figure 5c3). Vertically aligned single crystalline ZnO NW arrays can therefore be achieved by engineering the ZnO texture layer and the corresponding hole diameter in the patterned photoresist layer.

In summary, we have demonstrated an effective approach for controllable wafer-scale fabrication of ZnO nanowire (NW) arrays. Laser interference patterning is employed to control the position, size, and orientation of synthesized ZnO NWs, while a hydrothermal (HT) chemical method is used to control the morphology and material properties of NWs. More importantly, combinations of both the laser interference patterning and the HT method allow more available access to large-scale uniformly patterned nanostructures at a high-throughput rate and a substantially reduced cost, both in time and in equipment resources, providing an efficient approach for fabricating highly ordered one-dimensional nanostructures at wafer scale without using cleanroom technology. The development of textured ZnO seed layer for replacing single crystalline GaN and ZnO substrates cannot only reduce the cost but also extend the large-scale fabrication of vertically aligned ZnO NW arrays on substrates of other materials, such as polymers, Si, and glass. This combined large-scale nanofabrication approach paves the path toward integrating nanostructures into devices or technology platforms, which are compatible with state-of-the-art micro/nanofabrication technologies, for applications in energy harvesting, sensing, electronics, optoelectronics, piezotronics, and plasmonics.

**Acknowledgment.** Research was supported by DARPA (Army/AMCOM/REDSTONE AR, W31P4Q-08-1-0009), BES DOE (DE-FG02-07ER46394), KAUST Global Research Partnership, NSF (DMS0706436, CMMI 0403671), MANA WPI program from NIMS, Japan, and the Georgia Institute of Technology. The authors thank Dr. Jung-Il Hong and Shu Xiang for technical assistance and discussions on XRD measurements.

**Supporting Information Available.** Figures of LIL patterned growth of ZnO NW arrays on GaN substrate

showing different open hole periods and sizes. This material is available free of charge via the Internet at <http://pubs.acs.org>.

## REFERENCES AND NOTES

- (1) Tian, B. Z.; Zheng, X. L.; Kempa, T. J.; Fang, Y.; Yu, N. F.; Yu, G. H.; Huang, J. L.; Lieber, C. M. *Nature* **2007**, *449*, 885.
- (2) Wang, Z. L.; Song, J. H. *Science* **2006**, *312*, 242.
- (3) Law, M.; Greene, L. E.; Johnson, J. C.; Saykally, R.; Yang, P. D. *Nat. Mater.* **2005**, *4*, 455.
- (4) Kelzenberg, M. D.; Boettcher, S. W.; Petykiewicz, J. A.; Turner-Evans, D. B.; Putnam, M. C.; Warren, E. L.; Spurgeon, J. M.; Briggs, R. M.; Lewis, N. S.; Atwater, H. A. *Nat. Mater.* **2010**, *9*, 239.
- (5) Dresselhaus, M. S.; Chen, G.; Tang, M. Y.; Yang, R. G.; Lee, H.; Wang, D. Z.; Ren, Z. F.; Fleurial, J. P.; Gogna, P. *Adv. Mater.* **2007**, *19*, 1043.
- (6) Cui, Y.; Wei, Q. Q.; Park, H. K.; Lieber, C. M. *Science* **2001**, *293*, 1289.
- (7) Zhou, J.; Gu, Y. D.; Fei, P.; Mai, W. J.; Gao, Y. F.; Yang, R. S.; Bao, G.; Wang, Z. L. *Nano Lett.* **2008**, *8*, 3035.
- (8) Huang, M. H.; Mao, S.; Feick, H.; Yan, H. Q.; Wu, Y. Y.; Kind, H.; Weber, E.; Russo, R.; Yang, P. D. *Science* **2001**, *292*, 1897.
- (9) Gudiksen, M. S.; Lathon, L. J.; Wang, J.; Smith, D. C.; Lieber, C. M. *Nature* **2002**, *415*, 617.
- (10) Thelander, C.; Agarwal, P.; Brongersma, S.; Eymery, J.; Feiner, L. F.; Forchel, A.; Scheffler, M.; Riess, W.; Ohlsson, B. J.; Gosele, U.; Samuelson, L. *Mater. Today* **2006**, *9*, 28.
- (11) Cui, Y.; Lieber, C. M. *Science* **2001**, *291*, 851.
- (12) Lieber, C. M.; Wang, Z. L. *MRS Bull.* **2007**, *32*, 99.
- (13) Wang, M. C. P.; Gates, B. D. *Mater. Today* **2009**, *12*, 34.
- (14) Henzie, J.; Barton, J. E.; Stender, C. L.; Odom, T. W. *Acc. Chem. Res.* **2006**, *39*, 249.
- (15) Lao, C. S.; Liu, J.; Gao, P. X.; Zhang, L. Y.; Davidovic, D.; Tummala, R.; Wang, Z. L. *Nano Lett.* **2006**, *6*, 263.
- (16) Hangarter, C. M.; Myung, N. V. *Chem. Mater.* **2005**, *17*, 1320.
- (17) Huang, Y.; Duan, X. F.; Wei, Q. Q.; Lieber, C. M. *Science* **2001**, *291*, 630.
- (18) Heo, K.; Cho, E.; Yang, J. E.; Kim, M. H.; Lee, M.; Lee, B. Y.; Kwon, S. G.; Lee, M. S.; Jo, M. H.; Choi, H. J.; Hyeon, T.; Hong, S. *Nano Lett.* **2008**, *8*, 4523.
- (19) Chai, J.; Buriak, J. M. *ACS Nano* **2008**, *2*, 489.
- (20) Fan, Z. Y.; Ho, J. C.; Jacobson, Z. A.; Yerushalmi, R.; Alley, R. L.; Razavi, H.; Javey, A. *Nano Lett.* **2008**, *8*, 20.
- (21) Yu, G. H.; Cao, A. Y.; Lieber, C. M. *Nat. Nanotechnol.* **2007**, *2*, 372.
- (22) Pevzner, A.; Engel, Y.; Elnathan, R.; Ducobni, T.; Ben-Ishai, M.; Reddy, K.; Shpaisman, N.; Tsukernik, A.; Oksman, M.; Patolsky, F. *Nano Lett.* **2010**, *10*, 1202.
- (23) Xu, S.; Wei, Y.; Kirkham, M.; Liu, J.; Mai, W.; Davidovic, D.; Snyder, R. L.; Wang, Z. L. *J. Am. Chem. Soc.* **2008**, *130*, 14958.
- (24) Martensson, T.; Carlberg, P.; Borgstrom, M.; Montelius, L.; Seifert, W.; Samuelson, L. *Nano Lett.* **2004**, *4*, 699.
- (25) Wang, X. D.; Summers, C. J.; Wang, Z. L. *Nano Lett.* **2004**, *4*, 423.
- (26) Chong, T. C.; Hong, M. H.; Shi, L. P. *Laser Photonics Rev.* **2010**, *1*, 123.
- (27) Greene, L. E.; Goldberger, J.; Kim, F.; Johnson, J. C.; Zhang, Y. F.; Saykally, R. J.; Yang, P. D. *Angew. Chem., Int. Ed.* **2003**, *42*, 3031.
- (28) Coltrin, M. E.; Hsu, J. W. P.; Scrymgeour, D. A.; Creighton, J. R.; Simmons, N. C.; Matzke, C. M. *J. Cryst. Growth* **2008**, *310*, 584.
- (29) Xu, S.; Ding, Y.; Wei, Y. G.; Fang, H.; Shen, Y.; Sood, A. K.; Polla, D. L.; Wang, Z. L. *J. Am. Chem. Soc.* **2009**, *131*, 6670.